Article

Corrosion Inhibition of Expired Cefazolin Drug on Copper Metal in Dilute Hydrochloric Acid Solution: Practical and Theoretical Approaches

Raiedhah A. Alsaiari [1], Medhat M. Kamel [2,*] and Mervate M. Mohamed [1,2]

[1] Empty Quarter Research Centre, Department of Chemistry, Faculty of Science and Arts in Sharurah, Najran University, Sharurah 78362, Saudi Arabia; raalsayari@nu.edu.sa (R.A.A.); mervate71@gmail.com (M.M.M.)

[2] Department of Chemistry, Faculty of Science, Suez Canal University, Ismailia 41522, Egypt

[*] Correspondence: medhat_darwish@science.suez.edu.eg; Tel.: +20-1004482037; Fax: +20-643230416

Abstract: In this work, we studied the corrosion of Cu metal in 0.5 mol L^{-1} HCl and the inhibition effect of the expired Cefazolin drug. The inhibition efficiency (IE) of Cefazolin varied according to its concentration in solution. As the Cefazolin concentration increased to 300 ppm, the IE increased to 87% at 298 K and decreased to 78% as the temperature increased to 318 K. The expired drug functioned as a mixed–type inhibitor. The adsorption of the drug on the copper surface followed Temkin's adsorption model. The magnitudes of the standard free energy change (ΔG^o_{ads}) and adsorption equilibrium constant (K_{ads}) indicated the spontaneous nature and exothermicity of the adsorption process. Energy dispersive X-ray (EDX) and scanning electron microscopy (SEM) techniques showed that the drug molecules were strongly attached to the Cu surface. The electrochemical frequency modulation (EFM), potentiodynamic polarization (PP), and electrochemical impedance spectroscopy (EIS) results were in good agreement with the results of the weight loss (WL) method. The density functional tight–binding (DFTB) and Monte Carlo (MC) simulation results indicated that the expired drug bound to the copper surface through the lone pair of electrons of the heteroatoms as well as the π-electrons of the tetrazole ring. The adsorption energy between the drug and copper metal was –459.38 kJ mol^{-1}.

Keywords: expired Cefazolin; copper; corrosion inhibition; hydrochloric acid

1. Introduction

Corrosion negatively affects the performance of materials and structures. It causes most metallic structures to lose strength, performance, and appearance [1]. Corrosion has a significant harmful economic impact on different businesses and negative environmental repercussions. Corrosion contributes to operational risks and apparatus maintenance, leading to frequent partial and even complete process termination, which causes significant economic damage [2,3].

According to studies conducted all over the world, corrosion damage is extremely high; utilizing the right corrosion control techniques, such as coating, painting, using expensive alloys, and applying inhibitors, can reduce the total damage by 20–25% [4,5]. Inhibitors are frequently used in acidic media to prevent corrosion of the metals [6]. Under various circumstances, inhibitors are beneficial for the preservation of metals. The mode of action of the inhibitor accounts for this selectivity. Inhibitors are especially useful in closed systems where the harmful environment is recycled or held for some time [7–10].

Salt hydrolysis causes acid formation during crude oil cracking. This will cause a disastrous impact on machinery. Inhibitors are powerful tools to eliminate this damaging effect. To prevent the corrosion of metals in acid electrolytes, organic inhibitors are most frequently used [11–14].

Cu and its alloys offer superior qualities for various applications. They have widespread applications in valve systems, condensers, and exchangers. Also, they are employed in the architectural industry for objects such as doorknobs, rods, padlocks, and building fronts. Copper is resistant to corrosion in different chemical media, but it is sensitive to corrosion in hydrochloric acid solutions [15]. Diluted HCl solutions are frequently used to remove scales and other corrosion products from industrial equipment [16–18].

The use of pharmaceuticals as corrosion inhibitors has recently increased [19]. Because of their eco–quality, these drugs are superior to common inhibitors. Drugs have replaced the traditional poisonous corrosion inhibitors because they are safe and have little detrimental environmental effects. A drug is employed as a corrosion inhibitor according to the following three criteria: (a) the drug structure has donor atoms, such as O, N, and S; (b) the drug is eco–friendly and useful in biological systems; and (c) the drug is easily prepared and purified.

Undoubtedly, the bulk of pharmaceutical treatments are more expensive than the standard organic inhibitors used in the industry. Thus, it is economically useless to use a fresh curing agent as a corrosion inhibitor. Consequently, it makes sense to use the properties of expired drugs to limit corrosion. Even after their expiration dates, pharmaceuticals drugs keep at least 90% of their initial potency; however, due to professional constraints and liability concerns, their use was restricted for therapeutic purposes [20]. The use of expired drugs could overcome two more sensitive problems, e.g., reducing environmental pollution with drugs and decreasing drug disposal costs [21].

Scientists have recently employed expired drugs, such as Ampicillin [22], Antidiabetic [23], Herbal [24], Ampicillin and Flucloxacillin [25], Acyclovir and Omeprazole [26], Ceftin [27], Antihypertensive [28], Antifungal [29], 6–mercaptopurine and 6–thioguanine [30], Ciprofloxacin [31], Glucosamine [32], Flunarizine Hydrochloride [33], Amiodarone [34], Phenylphrine [35], Betamethasone [36], Podocip [37], Gentamycine [38], Lioresal [39], Midazolam [40], Fluoxymesterone [41], Atorvastin [42], etc., to inhibit the corrosion of different metals.

Cefazolin, a wider cephalosporin antibiotic, is employed for moderate–to–intense bacterial infections of the lungs, bones, joints, blood, heart valves, and urinary system, and skin infections. When given parenterally and orally to mice and rats, the antibiotic Cefazolin has relatively low acute toxicity. Cefazolin has no effect on the reproductive system, or the progeny of rats treated before and during mating, gestation, or breastfeeding. It is not teratogenic for mice or rabbits [43]. Cefazolin has various binding sites, including N, S, and O atoms. The ability of the drug to inhibit corrosion occurs via interaction with the metal surface through the adsorption process. Unexpired Cefazolin is more expensive than the tested organic inhibitors. Therefore, the focus of this study was on the use of expired Cefazolin as a corrosion inhibitor. According to this work, the expired Cefazolin drug can decrease the cost of disposal and the requirement for environment friendly products. This study used electrochemical and chemical techniques to assess the corrosion inhibition of Cu in a 0.5 mol L^{-1} HCl solution using expired Cefazolin. The drug is cheap and non–toxic [43]. To the best of our knowledge, no one has ever proposed using outdated Cefazolin drug to inhibit copper dissolution in HCl media.

This work aimed to study the impact of the expired Cefazolin drug on copper metal corrosion in a 0.5 mol L^{-1} HCl pickling solution. EIS, WL, EFM, and PP techniques were used to conduct the experiments. SEM and EDX techniques examined the morphology and composition of the copper metal surface. Different adsorption isotherms were utilized to assess the drug's adsorption type on copper metal. The thermodynamic parameters related to the adsorption process were also determined. DFTB, MC, and computational investigations described the interactions between the Cefazolin molecules and the copper metal surface.

2. Results and Discussion

2.1. WL Measurements

2.1.1. The Impact of Drug Concentration

The corrosion rate (k) and inhibition efficiency were determined for blank and different concentrations (50–300 ppm) of the expired Cefazolin drug using the WL method. WL measurements were used to assess Cefazolin's inhibition activity. Equation (1) is used to compute the corrosion rate (k) [44].

$$k = \frac{\Delta W}{At} \qquad (1)$$

where ΔW is the WL of the Cu sheet in mg, A is the area of the Cu sheet in cm^2, and t is the immersion time in minutes. Equation (2) is used to calculate the inhibition efficiency (IE_w) [45].

$$IE_w = \left(1 - \frac{W_{inh}}{W_{corr}}\right) \times 100 \qquad (2)$$

where W_{corr} and W_{inh} are the WL of Cu sheets without and with the drug, respectively. Table 1 shows WL data for copper metal in 0.5 mol L^{-1} HCl without and with different doses of the expired Cefazolin at different temperatures. The dissolution of copper to form the cuprous ion, Cu$^+$, causes the anodic reaction of Cu in HCl acid to occur rapidly [46].

$$Cu \rightarrow Cu^+ + e^- \text{ (fast)} \qquad (3)$$

Table 1. Data of WL measurements at 180 min for copper in 0.5 mol L^{-1} HCl, in the absence and presence of different concentrations of expired Cefazolin drug at different temperatures.

Temperature (K)	Dose of Drug (ppm)	Weight Loss (mg cm^{-2})	$k \times 10^{-3}$ (mg cm^{-2} min^{-1})	Surface Coverage θ	IE_w (%)
	0.00	8.50	11.8	–	–
	50	3.5	4.86	0.59	59 ± 0.2
	100	3	4.16	0.65	65 ± 0.1
298	150	2.7	3.75	0.68	68 ± 0.3
	200	1.9	2.64	0.78	78 ± 0.2
	250	1.5	2.08	0.82	82 ± 0.3
	300	1.1	1.50	0.87	87 ± 0.2
	0.00	9.1	12.6	–	–
	50	3.7	5.13	0.53	53 ± 0.3
	100	3.3	4.58	0.64	64 ± 0.5
303	150	3.1	4.30	0.66	66 ± 0.4
	200	2.2	3.05	0.76	76 ± 0.2
	250	1.65	2.28	0.82	82 ± 0.1
	300	1.3	1.81	0.86	86 ± 0.2
	0.00	11	15.2	–	–
	50	5.3	7.36	0.52	52 ± 0.5
	100	4.2	5.83	0.62	62 ± 0.6
308	150	3.9	5.41	0.65	65 ± 0.1
	200	2.9	4.03	0.74	74 ± 0.3
	250	2.3	3.19	0.79	79 ± 0.3
	300	1.9	2.63	0.83	83 ± 0.2
	0.00	16.5	22.9	–	–
	50	8.43	11.7	0.49	49 ± 0.3
	100	7.34	10.2	0.56	56 ± 0.1
318	150	6.33	8.79	0.62	62 ± 0.2
	200	5.28	7.33	0.68	62 ± 0.5
	250	4.67	6.48	0.61	61 ± 0.2
	300	3.55	4.93	0.78	78 ± 0.4

The cuprous ion reacts with the chloride ion in solution, and forms the insoluble CuCl, which precipitates on the Cu surface [47,48].

$$Cu^+ + Cl^- \rightarrow CuCl \tag{4}$$

The produced CuCl provides insufficient protection for the Cu surface because of its poor cohesion. It interacts with one other Cl^- ion to form the soluble chloride complex, $CuCl_2^-$.
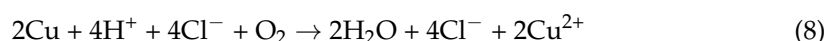
$$CuCl + Cl^- \rightarrow CuCl_2^- \tag{5}$$

The result is that copper corrodes. The soluble complex, however, could oxidize to cupric ions, Cu^{2+}.

$$CuCl_2^- \rightarrow Cu^{2+} + 2Cl^- + e \tag{6}$$

In oxygenated acidic chloride solutions, the cathodic reaction is:

$$4H^+ + O_2 + 4e \rightarrow 2H_2O \tag{7}$$

Consequently, copper in acid chloride solutions exhibits the overall corrosion reaction:

$$2Cu + 4H^+ + 4Cl^- + O_2 \rightarrow 2H_2O + 4Cl^- + 2Cu^{2+} \tag{8}$$

Contrarily, Figure 1 shows that the expired Cefazolin significantly decreases the WL of Cu metal in HCl solution. The adsorption of the drug molecules on the Cu surface suppresses the tendency of copper to dissolve and reduces the rate of corrosion. When the drug is present at a concentration of 300 ppm, IE_w reaches 87% at 298 K. This clarifies that the expired Cefazolin may effectively inhibit the corrosion of Cu metal in HCl solution.
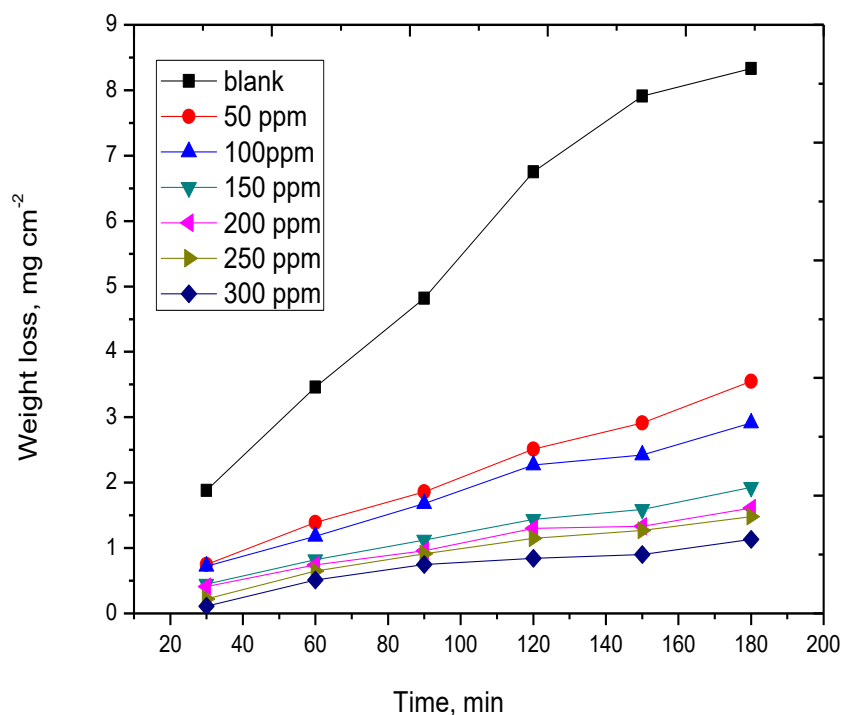

Figure 1. WL curves of copper metal in 0.5 mol L^{-1} HCl without and with distinct concentrations of expired Cefazolin at 298 K.

2.1.2. Impact of Temperature on Inhibition Efficiency

It is quite challenging to foresee how temperature will affect the inhibited acid–metal reaction because of the different changes on the metal surface. These alterations can take different forms, including quick etching, desorption of the inhibitor, and the inhibitor's

own breakdown or restructuring [49]. Both *k* and IE_w are measured in the temperature range (298–318 K). Table 1 displays the impact of temperature on *IE* and *k*. In the presence or absence of different dosages of the expired antibiotic, the increase in temperature results in an increase in the corrosion rate of Cu metal. This could result from the increased impact of rising temperatures on the rate of electrochemical reactions.

According to the data in Table 1, IE_w decreases as the temperature increases. Desorption of the drug molecules from the Cu surface will be the cause [50]. This result clearly shows that the studied drug attaches to the Cu surface in a physical form of adsorption since the rate of the desorption process increases with increasing temperature.

2.2. Adsorption Type and Chemical Thermodynamics Approach

The ability of heterocyclic compounds to adsorb on a metal surface and create a protective film is the main cause of the corrosion inhibition. The double–layer structure is disturbed by the interaction of anticorrosion molecules with the metal surface, which may cause the water molecules at the metal–electrolyte interface to reorganize as follows:

$$Drug_{(soln.)} + H_2O_{(ads)} \rightarrow Drug_{(ads)} + H_2O_{(soln.)} \tag{9}$$
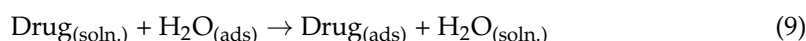
It is crucial to identify the isotherms that describe the adsorption behavior of corrosion inhibitors because it reveals the type of interaction between the metal and the inhibitor [51]. As a result, different adsorption isotherms, including Temkin, Langmuir, and Freundlich, are investigated (Figures 2–4); the isotherm that best fits the surface coverage data is shown as the most representative. Typically, the highest regression coefficient R^2 indicates the best fit. Plotting the surface covering (θ) data is performed using the measured WL data. Upon conducting a comprehensive analysis of the fitting of different adsorption isotherms, the Temkin model is found to exhibit the best linear regression, with $R^2 \geq 0.991$ (according to Figure 2) [52]. In this instance, the adsorption mechanism is best described by the Temkin isotherm.
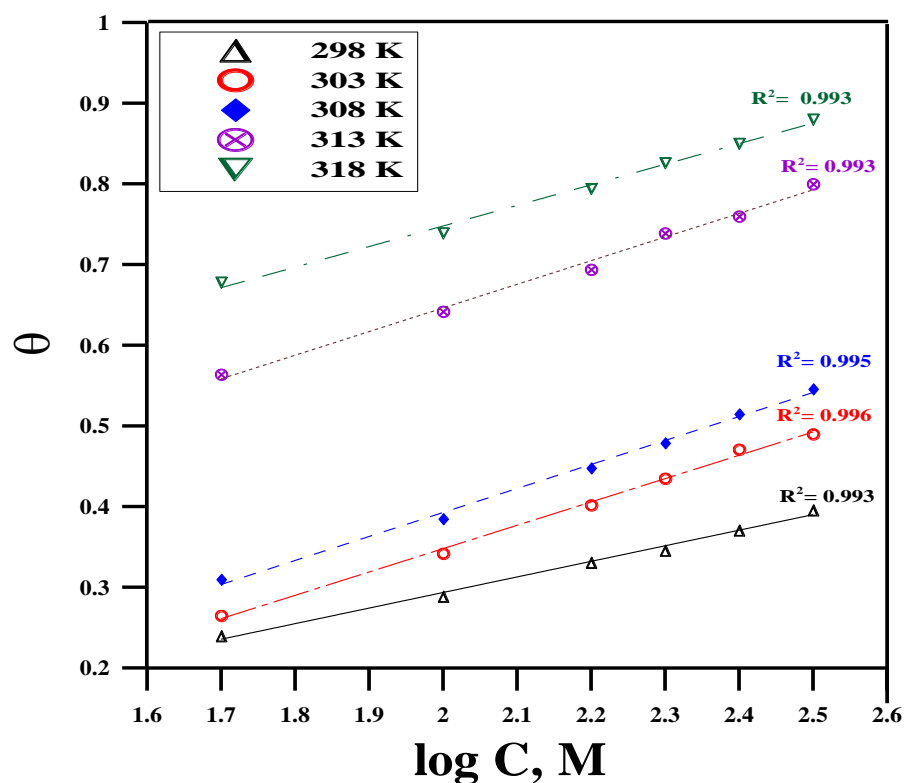

Figure 2. Temkin's model at different concentrations of expired Cefazolin at different temperatures for copper metal in 0.5 mol L^{-1} HCl solution.
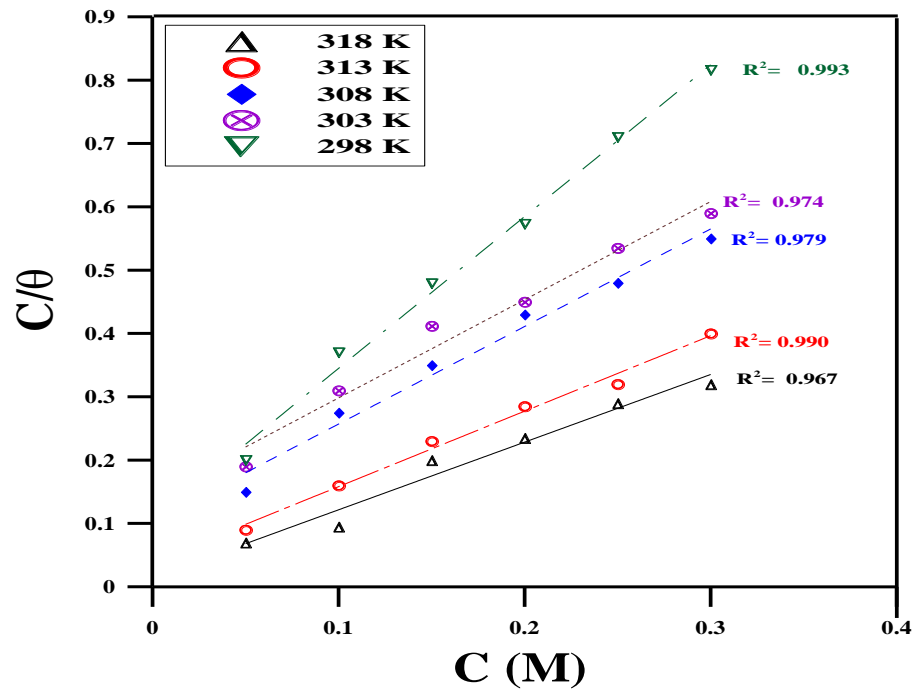
Figure 3. Langmuir's model at different concentrations of expired Cefazolin at different temperatures for copper metal in 0.5 mol L^{-1} HCl solution.
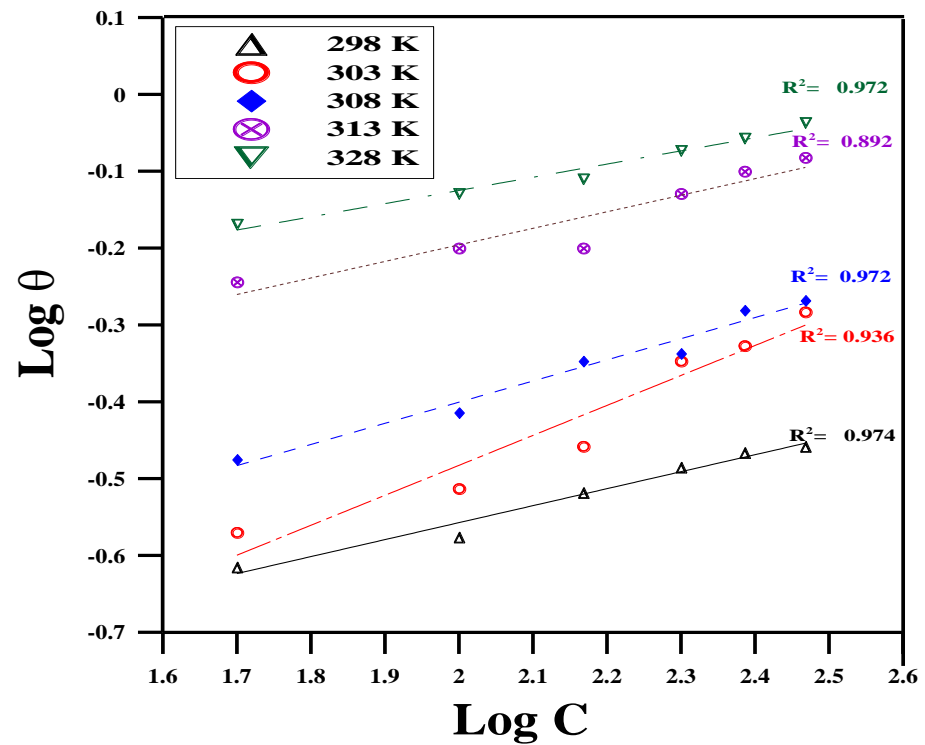

Figure 4. Freundlich's model at different concentrations of expired Cefazolin at different temperatures for copper metal in 0.5 mol L^{-1} HCl solution.

According to Temkin's model, Equation (10) correlates $\theta_{coverage}$ to the equilibrium constant (K_{ads}) for the adsorption process [53].

$$\theta_{coverage} = \frac{2.303}{a}\, logK_{ads} + \frac{2.303}{a} logC \tag{10}$$

where θ is the fraction of surface coverage ($\theta = IE_w/100$), K_{ads} is the equilibrium constant, C is the drug's concentration, and "a" is a molecular interaction parameter. A straight line of a slope $\frac{2.303}{a}$ and an intercept of $\frac{2.303}{a} \log K_{ads}$ are obtained by drawing a relationship between θ and $\log C$.

Table 2 estimates and summarizes the K_{ads} magnitudes. At lower temperatures, the values of K_{ads} are high, indicating that the drug is strongly adsorbed on the Cu surface. The desorption rate of the antibiotic molecules increases with increasing temperature, which causes the values of K_{ads} to decrease. The standard Gibbs free energy ($\Delta G^o{}_{ads}$), which is derived from Equation (11), is another parameter related to the adsorption constant (K_{ads}) [54,55].

$$\Delta G^o_{ads} = -RT \ln(55.5\, K_{ads}) \tag{11}$$

Table 2. Adsorption parameters for copper at various concentrations of expired Cefazolin at different temperatures in 0.5 mol L^{-1} HCl solution.

Temperature (K)	K_{ads} (L mol^{-1})	$-\Delta G^o{}_{ads}$ (kJ mol^{-1})
298	15.14	16.68
303	7.59	15.22
308	3.55	13.53
313	2.82	13.15
318	2.29	12.81

The estimated values of $\Delta G^o{}_{ads}$ are between -12.81 and -16.68 kJ mol^{-1}, showing that the drug is physically adsorbed on copper metal at the temperatures used. The finding that IE_w decreases with increasing temperature supports this conclusion. The negative magnitudes of $\Delta G^o{}_{ads}$ signify the stable state of the adsorbed film on the CS surface as well as the spontaneous action of the separated molecules during the adsorption process [56]. The presence of heteroatoms and π–electrons in the structure of the expired drug may be responsible for its interaction with the copper surface.

2.3. PP Measurements

Figure 5 shows copper polarization curves in 0.5 mol L^{-1} HCl without and with distinct dosages of the antibiotic Cefazolin. The corrosion current (i_{corr}) markedly decreases as the Cefazolin concentration increases. Therefore, the antibiotic can successfully inhibit copper metal corrosion in an acidic medium. The cathodic polarization curves in Figure 5 have a consistent trend, showing that Cefazolin's adsorption on the copper surface has no effect on the cathodic reaction mechanism. In the presence of Cefazolin, the slopes of the anodic curves have changed, suggesting that the mechanism of the anodic reaction has altered. The Tafel extrapolation method is used to determine E_{corr} and i_{corr} [12]. The results are shown in Table 3. Equation (12) is used to calculate the corrosion current, i_{corr}.

$$i_{corr} = B/R_p \tag{12}$$

where R_p is the polarization resistance and B is a constant related to Stern and Geary. B is calculated according to the relationship:

$$B = \frac{\beta_a \cdot \beta_c}{2.303(\beta_a + \beta_c)} \tag{13}$$

where β_a and β_c, respectively, are the anodic and cathodic Tafel constants. The following equation is used to compute IE_p.

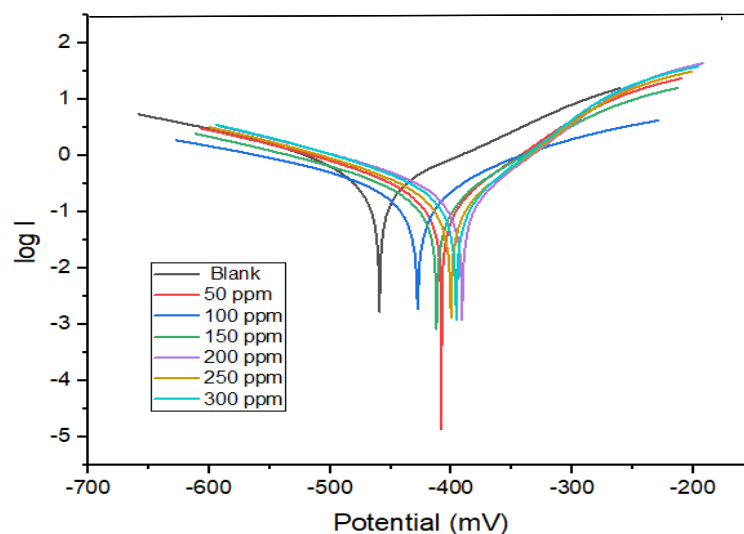$$IE_p = \left(1 - \frac{i_{(inh)}}{i_{(free)}}\right) \times 100 \tag{14}$$

Figure 5. PP for the corrosion of copper in 0.5 mol L^{-1} HCl without and with different concentrations of expired Cefazolin at 298 K.

Table 3. PP data of copper in 0.5 mol L^{-1} HCl containing different concentrations of expired Cefazolin at 298 K.

Concentration (ppm)	$-E_{corr} \times 10^{-3}$ (V/SCE)	$i_{corr} \times 10^{-6}$ (A cm^{-2})	$\beta_a \times 10^{-3}$ (V dec^{-1})	$-\beta_c \times 10^{-3}$ (V dec^{-1})	IE_p (%)
Blank	420	542	115	136	–
50	415	240	122	125	55.7 ± 0.1
100	403	212	116	133	60.9 ± 0.3
150	395	165	107	118	69.6 ± 0.3
200	388	134	114	127	75.2 ± 0.2
250	380	108	105	134	80.1 ± 0.2
300	372	78	98	119	85.6 ± 0.1

$i_{(free)}$ and $i_{(inh)}$ are the corrosion current densities in the absence and presence of the drug, respectively. In accordance with Table 3, E_{corr} is −420 mV (SCE) for the blank solution. The corrosion potential changes to a less negative value after the addition of Cefazolin, but without a clear trend. This indicates that Cefazolin functions as a mixed–type inhibitor in 0.5 mol L^{-1} HCl, forming an adsorbed film at the metal/solution boundary that decreases the available anodic and cathodic sites. Cefazolin antibiotic serves as a mixed–type corrosion inhibitor as the maximum change in corrosion potential caused by the drug is less than 85 mV [57]. This indicates that both half–reactions (anodic and cathodic) are altered by the addition of the expired drug. The cathodic Tafel slopes change greater than the anodic Tafel slopes, implying that Cefazolin molecules are adsorbed on both sites but preferentially under cathodic control, which inhibits the cathodic reduction reaction and anodic dissolution [56].

2.4. EIS Study

EIS provides considerable mechanistic and kinetic details for the electrochemical system under investigation. EIS measures the ability of a circuit to counteract the flowing electrical current. It is established by exposing the electrochemical cell to an AC potential and measuring the result in the cell. EIS offers an alternative technique for describing the adsorbed film on the electrode that is illustrated by the charge transfer resistance (R_{ct}). It has been shown that the interface capacitance can be used to evaluate the film quality [58].

Figure 6a,b displays the Nyquist and Bode plots for the Cu in 0.5 mol L^{-1} HCl with different Cefazolin dosages at 298 K. The impedance spectra of copper have a low–frequency inductive loop and a high–frequency capacitive loop, except at concentrations greater than

200 ppm. The time constant and charge transfer reaction of the electrical double layer is responsible for the high–frequency capacitive loop. At high frequencies, the surface film formation could be the cause of the time constant. However, the inductive loop has been related to a disintegration process, bulk relaxation process, or surface relaxation process [56]. The relaxation process caused by the adsorption of species like H_{ads} and Cl^- on the copper surface may be the cause of the low–frequency inductive loop in the inhibited acid solution containing a lower Cefazolin concentration. It could possibly be related to the passivated surface's re–dissolution at low frequencies. Our opinion is supported by the fact that this semicircle disappears when a higher concentration of Cefazolin is added [56]. The diameter of the capacitance loop increases significantly as the dose of the Cefazolin drug increases in the corrosive medium (Figure 6a). This indicates that the antibiotic Cefazolin, which has a considerable inhibitory effect on the corrosion of copper, adsorbs and increases the charge transfer resistance (R_{ct}). As the concentration of the drug increases in the solution, the semicircle's diameter grows larger. This demonstrates that the electron transfer step is the slowest step throughout the corrosion process. Regarding what the EIS theory predicted, the loops in the high–frequency range are not idealized semicircles. This discrepancy may be attributed to the unsatisfactory performance of the double layer as a capacitor.

The imperfect effectiveness is assigned to the frequency dispersion, which is caused by the roughness and non–homogeneity of the surface.

The capacitive reactance modulus in the Bode plot increases by an order of magnitude in the low-frequency zone, as displayed in Figure 6b. Additionally, the slope of the impedance modulus is nearly one, and the phase angle attains $-65°$ in the domain of intermediate frequency. This implies that the copper capacitance feature of Cefazolin is indeed present. When Cefazolin adsorbs on the surface of copper, it only creates a time constant, as can be observed in Figure 6b, where only one peak can be seen inside the phase angle. Figure 6c depicts the analogous Randles circuit. The circuit shows that the double–layer capacitance C_{dl} and R_{ct} are linked in parallel. Both outputs are linked in series with the solution resistance, R_s. The practical findings are in good accord with this concept. Equation (15) is utilized to estimate IE_s using R_{ct} [59,60].

$$IE_s = \frac{R_{ct} - R_{ct}^o}{R_{ct}} \times 100 \qquad (15)$$

where R_{ct}^o and R_{ct}, respectively, stand for charge transfer resistance without and with the drug. The impedance characteristics are listed in Table 4. As the antibiotic concentration increases, R_{ct} increases; however, C_{dl} decreases. The antibiotic molecules gradually replace the water molecules at the Cu surface. As a result, the dissolution response will be minimized [61]. The dissolution of the metal slows down as the R_{ct} values increase [53].

Table 4. EIS data of copper in 0.5 mol L^{-1} HCl in the absence and presence of different concentrations of expired Cefazolin at 298 K.

Concentration (ppm)	$C_{dl} \times 10^{-6}$ (F cm^{-2})	R_{ct} (Ω cm^2)	θ	IE_s (%)
Blank	343	55.4	−	−
50	163.5	130.7	0.58	58 ± 0.3
100	155.1	170.5	0.77	77 ± 0.3
150	142.4	220.3	0.75	75 ± 0.4
200	104.8	270.8	0.80	80 ± 0.1
250	88.7	355.6	0.84	84 ± 0.2
300	68.9	487	0.89	89 ± 0.2

The reduction in C_{dl} values is attributed to a decrease in the dielectric constant, other than the increasing thickness of the electrical double layer. This finding suggests that the drug molecules work at the metal surface through adsorption [62]. The interaction of the antibiotic with previously adsorbed Cl^- ions causes the adsorption to take place. As an

alternative, the interaction could occur between the π–electrons of antibiotic molecules or unpaired electrons and the vacant orbitals of the metal [63].
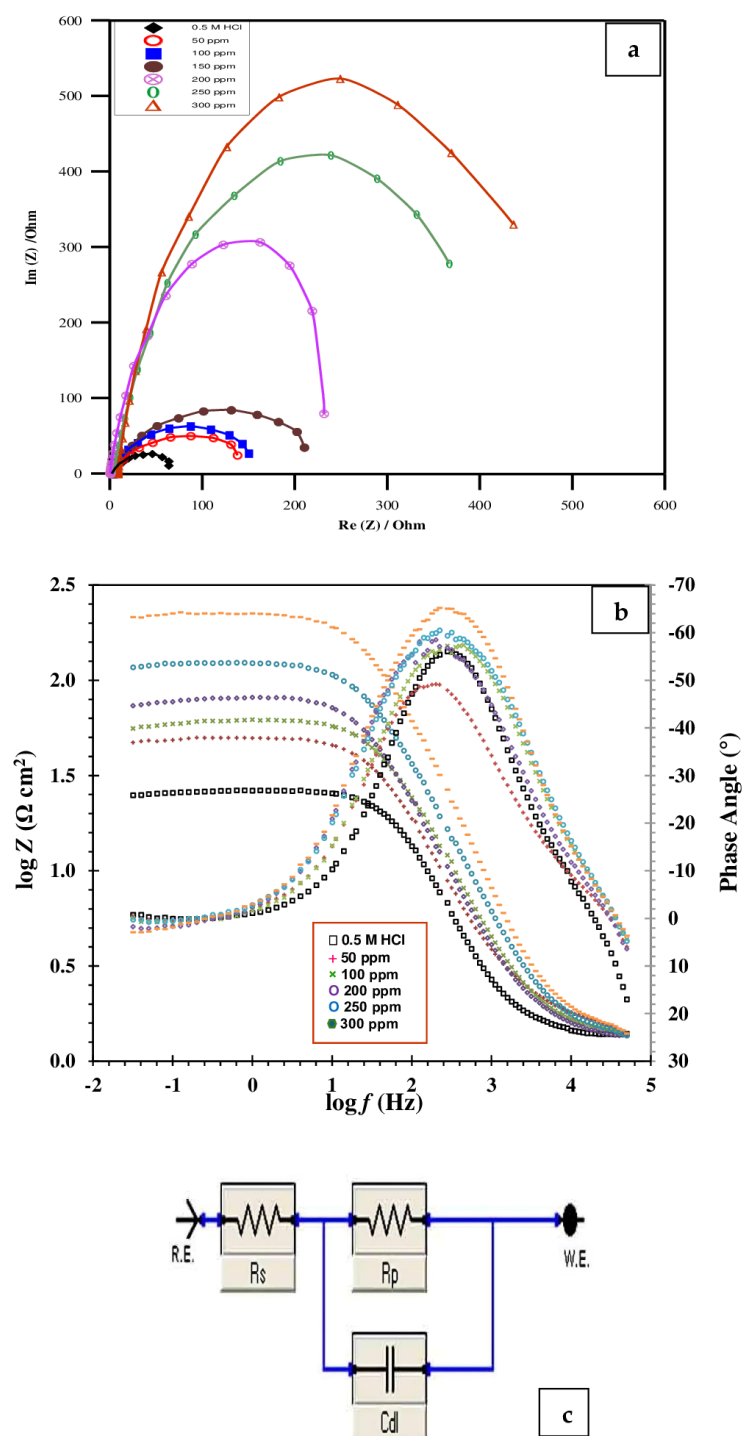

Figure 6. Nyquist (**a**) and Bode (**b**) plots and electrochemical equivalent circuit (**c**) for the corrosion of copper in 0.5 mol L^{-1} HCl without and with different concentrations of expired Cefazolin at 298 K.

2.5. EFM Study

It is possible to calculate the instantaneous rate of corrosion by using the EFM technique. This can be achieved with a small polarizing signal and without previous knowledge of the Tafel characteristics. The EFM technique can track variations in the environment's corrosiveness, such as changes in oxygen content and hydrodynamic circumstances. The

EFM approach is a prime choice for online corrosion monitoring applications because of its benefits, such as direct nondestructive rapid measurement of corrosion rates and data validation [45]. Figure 7 shows the modulation spectra obtained from EFM testing for the dissolution of copper in a 0.5 mol L^{-1} HCl solution without and with different doses of expired Cefazolin. The current response includes both the input frequencies and frequency components. The latter results from the multiples, differences, and sum of the two input frequencies. As a result of the excitation frequencies, there are two main peaks at 0.2 and 0.5 Hz.
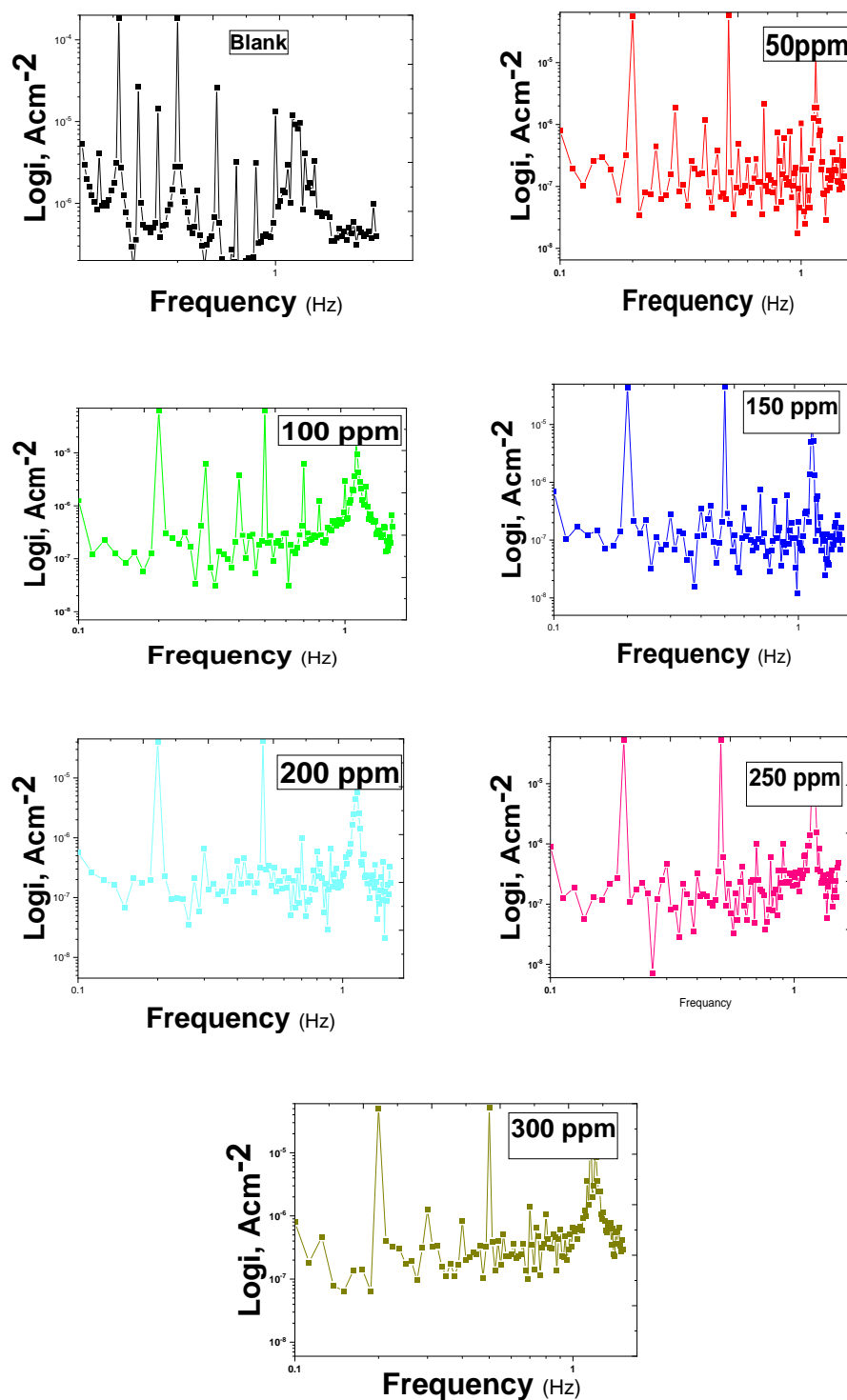

Figure 7. EFM spectra for the corrosion of copper in 0.5 mol L^{-1} HCl without and with distinct concentrations of expired Cefazolin at 298 K.

The Tafel slopes, the corrosion current, and the causality factors (CF–2, CF–3) are computed using the two main peaks. The peaks between 1 and 20 μA indicate the harmonics, summation, and differences between the two excitation frequencies. Table 5 displays the corrosion kinetic characteristics, including IE_{EFM}, i_{corr}, Tafel parameters, and causality factors. The corrosion current density decreases as the drug concentration increases. As the concentration of Cefazolin increases, the effectiveness of the inhibition increases. The causality factors are quite close to their predicted ones (Table 5). According to EFM theory, this could guarantee the accuracy of the Tafel parameters and corrosion current densities. [45]. Equation (16) provides IE_{EFM} calculations based on the EFM data.

$$IE_{EFM} = \frac{i_{corr}^{\circ} - i_{corr}}{i_{corr}^{\circ}} \times 100 \tag{16}$$

where i_{corr}° and i_{corr} are the corrosion current densities in the absence and presence of the drug, respectively.

Table 5. Electrochemical kinetic parameters obtained by EFM technique for copper metal in 0.5 mol L^{-1} HCl in the absence and presence of different concentrations of expired Cefazolin at 298 K.

Concentration (ppm)	$i_{corr} \times 10^{-6}$ (A cm^{-2})	$\beta_a \times 10^{-3}$ (V dec^{-1})	$-\beta_c \times 10^{-3}$ (V dec^{-1})	CF–2	CF–3	IE_{EFM} (%)
Blank	542	112	124	1.95	3.09	–
50	230	122	133	2.02	3.03	57.6 ± 0.2
100	206	113	215	1.98	2.98	61.2 ± 0.3
150	160	126	186	1.94	2.89	70.4 ± 0.1
200	128	98	154	2.08	3.06	76.4 ± 0.2
250	105	114	164	2.01	3.04	80.6 ± 0.2
300	80	99	145	1.96	2.93	85.1 ± 0.3

2.6. SEM and EDX Studies

The existence of a protective film of the expired drug on the Cu surface is further clarified by the SEM technique. Additionally, EDX studies are performed to check whether the drug is attached to Cu or not. SEM micrographs of the polished Cu and Cu immersed in a 0.5 mol L^{-1} HCl solution without and with 300 ppm of the Cefazolin antibiotic are shown in Figure 8. To initiate the corrosion process, many scratches are left on the surface of the polished copper, as shown in Figure 8a [26]. After being in contact with a 0.5 mol L^{-1} HCl solution for 8 h, the morphology of the copper surface is shown in Figure 8b. The entire Cu surface has deteriorated because of the pitting impact of the chloride ions in solution. As shown in Figure 8c, the expired drug effectively improves the surface morphology of copper because of its ability to form a protective film on the surface of copper metal.

The presence of the drug molecules on the Cu surface is confirmed using the EDX technique. Figure 9 shows the corresponding EDX spectra. Both copper and chloride peaks can be seen for the samples that are exposed to the blank solution because $CuCl_2$ is formed at the copper surface (Figure 9a). For samples that have been exposed to the expired drug, C, N, and O peaks can be observed in the EDX pattern (Figure 9b). This result reveals the adsorption of the drug molecules on the copper surface, showing a significant inhibition of the Cu corrosion. There is no peak for S. This indicates that the concentration of S is too small to be detected on the copper surface. The presence of the C, N, and O atoms on the metal surface suggests that the drug molecules are strongly adsorbed on the copper, forming a protective film. The formed film protects the copper from corrosion.
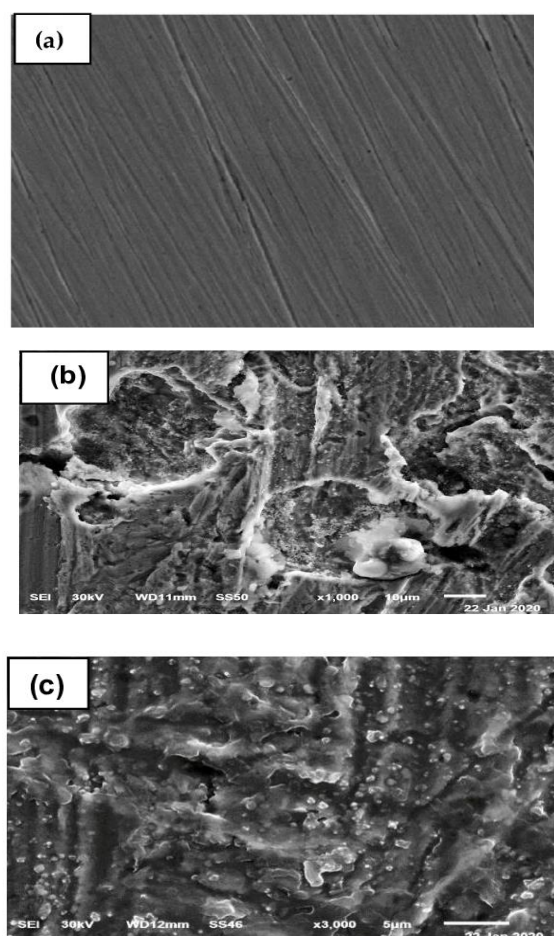
Figure 8. SEM micrographs of polishing copper (**a**), copper after 8 h of immersion in 0.5 mol L^{-1} HCl without (**b**) and with (**c**) 300 ppm of expired Cefazolin at 298 K.
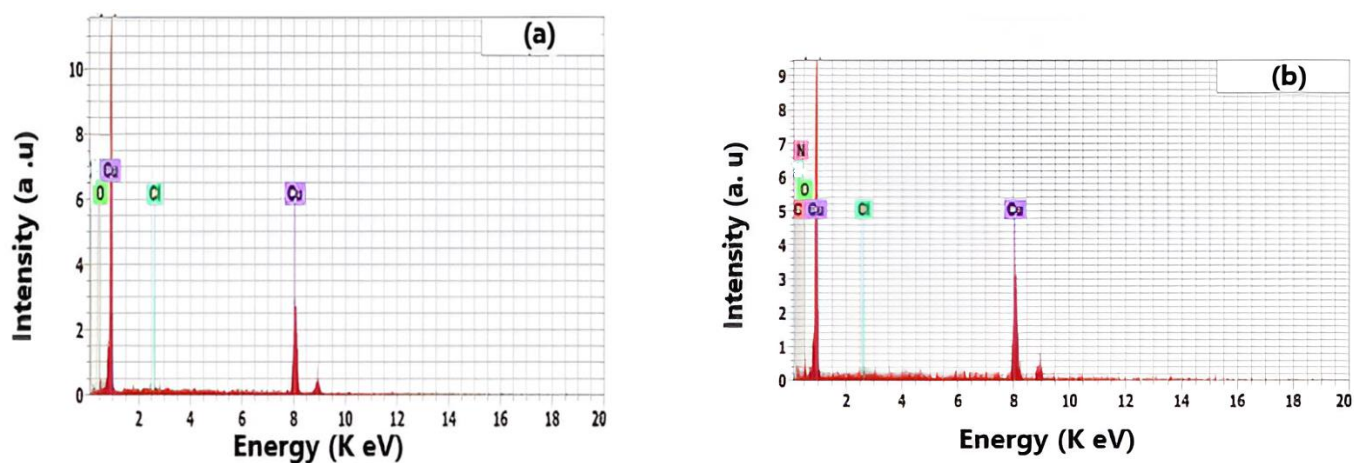

Figure 9. EDX analysis of copper after 8 h of immersion in 0.5 mol L^{-1} HCl without (**a**) and with (**b**) 300 ppm of Cefazolin at 298 K.

2.7. Quantum Chemical Calculations

2.7.1. DFTB Results

Density functional tight–binding (DFTB) calculations can provide valuable information on the electronic and thermodynamic properties of corrosion inhibitors. The HOMO–LUMO energy gap (ΔE) and other quantum chemical characteristics, such as the LUMO and HOMO energy levels, are utilized to explain the efficiency of Cefazolin's inhibition.

The HOMO and LUMO energies are found to be -6.40 and -2.01, respectively, suggesting that the Cefazolin drug can function as an electron donor, which facilitates the formation of a protective film on the copper surface. The calculated ΔE value of 4.39 shows that Cefazolin has good stability and can effectively inhibit the corrosion process (Table 6).

Table 6. The calculated quantum chemical parameters obtained from DFT theory for Cefazolin molecule.

HOMO (au)	LUMO (au)	ΔE (au)	I (au)	A (au)	η (au)	σ (au)$^{-1}$	μ (au)	χ (au)	ω (au)	ε (au)	ΔN_{max} (au)
-6.40	-2.01	4.39	6.4	2.01	2.19	0.46	-4.21	4.21	4.04	0.25	1.92

According to the distribution of the HOMO electron density, the drug molecule can donate electrons to the Cu metal through the adsorption sites of the tetrazole ring (a five–membered ring made up of four nitrogen atoms and one carbon atom), as well as π–orbitals and hetero N atoms (Figure 10). However, the distribution of the LUMO electron density suggests that the drug molecule can accept electrons from the copper metal via the dithiazole ring and 5–thia–1–azabicyclo[4.2.0]oct–2–ene–2–carboxylic acid [64,65].
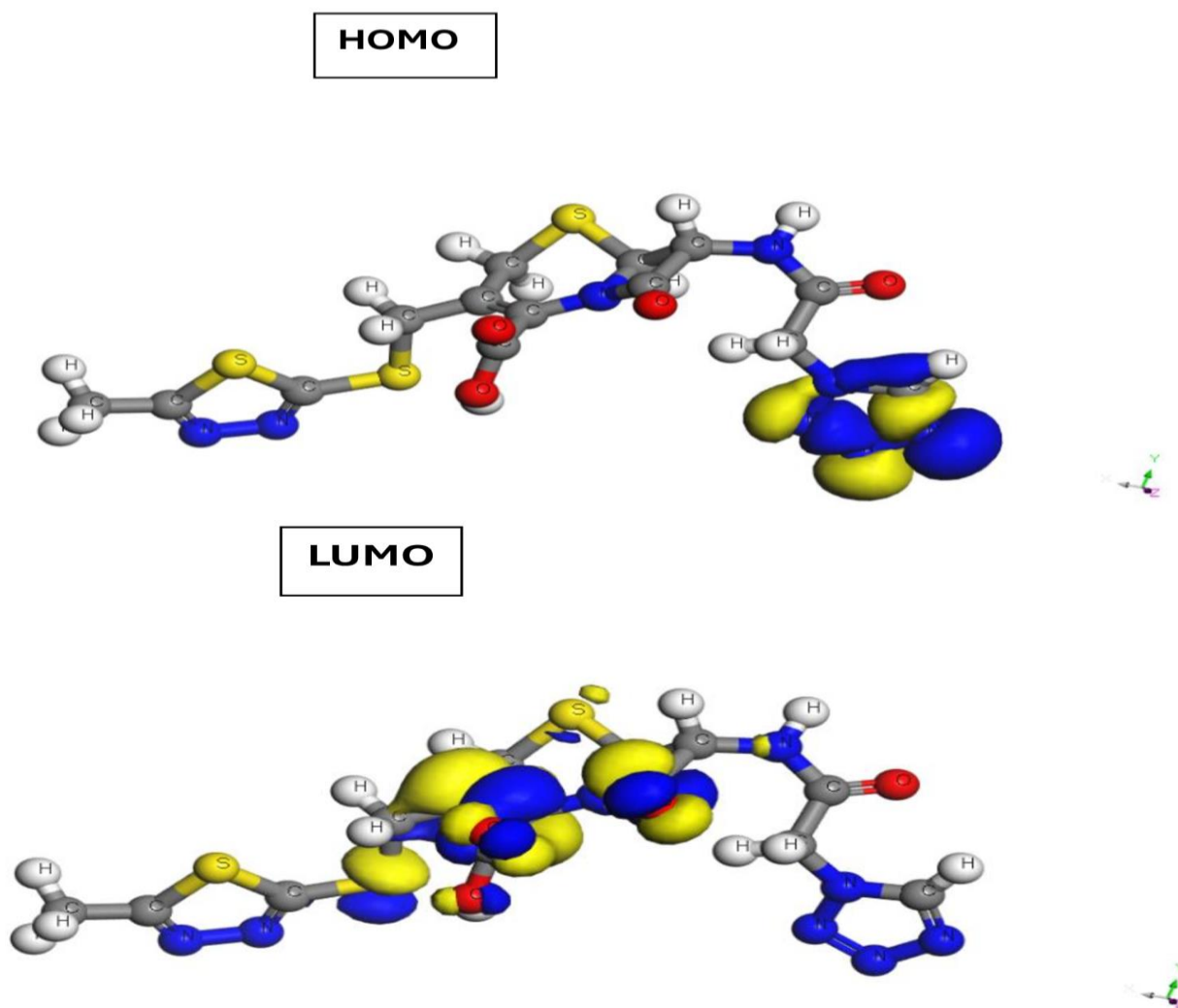

Figure 10. Molecular orbitals: HOMO and LUMO of Cefazolin drug.

Figure 11 shows the electron density plots of the Cefazolin drug. The molecular electrostatic potential (MEP) mapping of the drug Cefazolin indicates that the tetrazole ring

is the nucleophilic center (the red region) for adsorption. This will improve the possibility of the adsorption process and create a protective film on the metal surface, increasing the effectiveness of inhibition. The electron density, which disperses throughout the entire molecule, strengthens the molecule's adsorption intensity over the copper surface. The hydrophobic carbon chain supports the attachment of adsorbed molecules by repelling aggressive chloride anions farther from the surface [66].
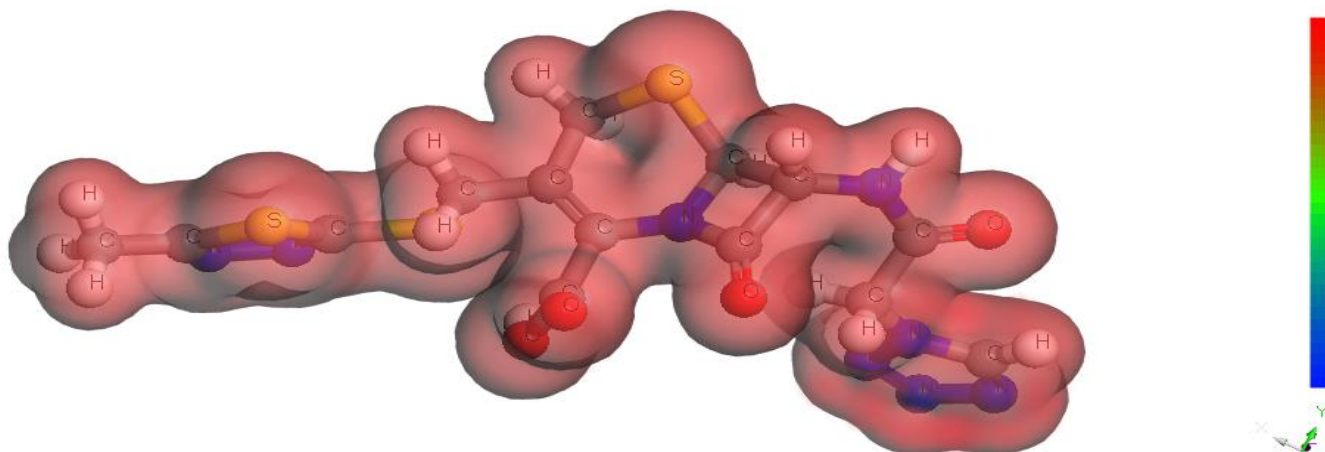

Figure 11. Electron density plots of the Cefazolin molecule.

Several descriptors can be calculated from the DFTB results, which assess the inhibition performance of the drug. They can be computed from the highest occupied molecular orbital energy (E_{HOMO}) and the lowest unoccupied molecular orbital energy (E_{LUMO}). Based on the literature [67], Table 6 reports the electronic parameters for the energy gap (ΔE), ionization potential (I), electron affinity (A), chemical potential (μ) electronegativity (χ), global hardness (η), softness (σ), electrophilicity index (ω), nucleophilicity (ε), and proportion of electron transfer (ΔN_{max}). The parameters are calculated according to the following relations [12]:

$$\Delta E = E_{\text{LUMO}} - E_{\text{HOMO}} \tag{17}$$

$$I = -E_{\text{HOMO}} \tag{18}$$

$$A = -E_{\text{LUMO}} \tag{19}$$

$$\mu = -\chi \tag{20}$$

$$\mu = \frac{(E_{\text{HOMO}} + E_{\text{LUMO}})}{2} \tag{21}$$

$$\eta = \frac{(E_{\text{LUMO}} - E_{\text{HOMO}})}{2} \tag{22}$$

$$\sigma = \frac{1}{\eta} \tag{23}$$

$$\Delta N_{max} = \frac{-\mu}{\eta} \tag{24}$$

$$\omega = \frac{\mu^2}{2\eta} \tag{25}$$

$$\varepsilon = \frac{1}{\omega} \tag{26}$$

The ionization potential of molecules expresses their chemical reactivity. Smaller ionization energy values indicate greater reactivity of the atoms and molecules in contrast

to large values, which indicate great stability of the molecules [68]. Table 6 indicates that Cefazolin has a strong inhibitory efficiency because of its low ionization energy value.

The χ value of the Cefazolin drug is a significant factor to be considered when evaluating its reactivity. The value indicates the degree to which it may keep electrons [69]. A small value of σ and a high value of η confirm a significant interaction between Cefazolin and the copper metal. [14]. The electrophilicity (ω) value of the Cefazolin molecule demonstrates stability. The reciprocal of electrophilicity provides nucleophilicity (ϵ). The estimated ΔN_{max} value for Cefazolin is 1.92, suggesting that it can release electrons, confirming the formation of a protective film on the copper surface [70]. According to quantum simulations, the current inhibitor has effective adsorption sites that can easily adsorb on the copper surface and form a protective film.

2.7.2. Monte Carlo Simulation (MC)

Monte Carlo simulations are used to study the interaction between a single drug molecule and the copper surface. MC modeling is a widely used computational technique for simulating the adsorption behavior of molecules on solid surfaces, including corrosion inhibitors. It can provide insights into the adsorption thermodynamics and kinetics, as well as the spatial arrangement of adsorbed molecules on the surface. The MC results show that Cefazolin exhibits favorable adsorption on the metal surface with a negative adsorption energy, indicating spontaneous adsorption. Figure 12 shows the side and top views of the most stable adsorption configuration of the Cefazolin molecule on the surface of copper. It is apparent from the side view of the optimized structure (Figure 12a) that the Cefazolin drug is adsorbed parallel to the Cu (111) surface via the donation of a lone pair of heteroatoms and π–electrons of the tetrazole ring to the copper metal [71]. A top–view image of the optimized structure shows that the Cefazolin molecule highly covers the copper surface (Figure 12b).
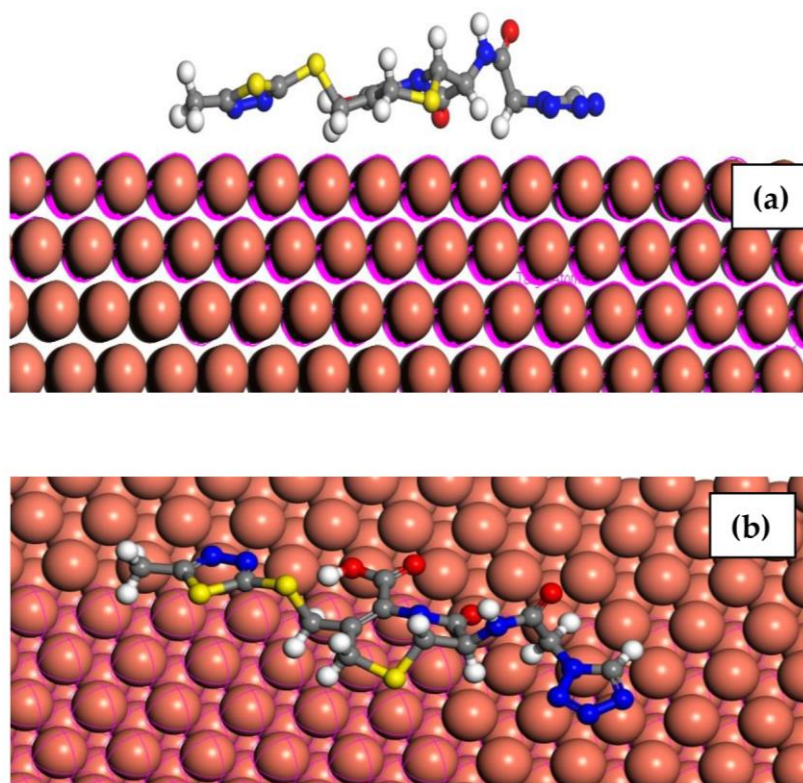

Figure 12. Side view (**a**) and top view (**b**) for the adsorption of the Cefazolin drug on copper surface.

The adsorption, deformation, and rigid adsorption energies are calculated as shown in Table 7. The adsorption energy, E_{ads}, is calculated according to Equation (27).

$$E_{ads} = E_{Cu-inh} - (E_{inh} - E_{Cu}) \tag{27}$$

where E_{inh}, and E_{Cu} are the total energy of the inhibitor and the copper surface, respectively. The Cu(111) surface energy is assumed to be zero [72]. The adsorption energy is the energy evolved or absorbed when the relaxed drug molecule is adsorbed on the copper surface. It is the sum of the rigid adsorption energy and the deformation energy of the drug molecule. The rigid adsorption energy reports the energy released or absorbed when the unrelaxed drug molecule is adsorbed on the copper. The deformation energy is the energy released when the adsorbed adsorbate molecule is relaxed on the copper surface [72]. The adsorption energy is found to be -459.38 kJ mol^{-1}. The negative E_{ads} value indicates that the adsorption is an energetically feasible process. A high adsorption energy value suggests that the Cefazolin molecule is a possible efficient inhibitor.

Table 7. The descriptors calculated by the Monte Carlo simulation for the adsorption of the Cefazolin drug on the Cu surface.

Total Energy (kJ mol^{-1})	Adsorption Energy (kJ mol^{-1})	Rigid Adsorption Energy (kJ mol^{-1})	Deformation Energy (kJ mol^{-1})
-598.67	-459.38	-453.32	-6.06

2.8. Mechanism of Corrosion Inhibition

According to Table 2, the calculated values of ΔG^o_{ads} are -12.81 to -16.68 kJ mol^{-1}, indicating that physisorption is the process by which the examined drug binds to copper metal in a solution of 0.5 mol L^{-1} HCl. This result is supported because inhibition efficiency decreases as the temperature increases. The presence of N, O, and π–electrons in the structure of the examined drug may be responsible for its interaction with the copper surface. According to Equations (3) and (7), O_2 and H$^+$ in the solution are mixed to form water at the cathode, while Cu metal is oxidized to Cu$^+$ at the anode. In addition, the Cefazolin molecule accepts electrons from the copper metal through the dithiazole ring and 5–thia–1–azabicyclo[4.2.0]oct–2–ene–2–carboxylic acid. The MC results confirm this. The proposed mechanism of inhibition is illustrated in Figure 13.
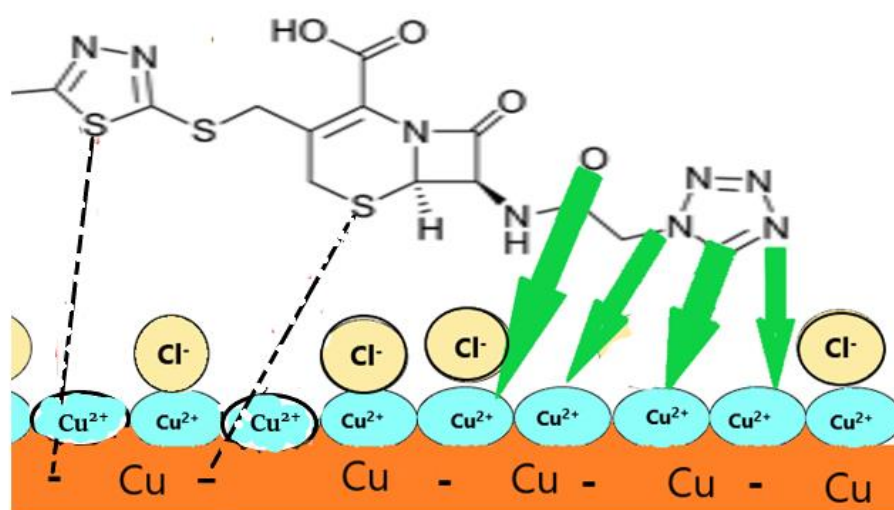

Figure 13. Proposed mechanism of the Cefazolin as corrosion inhibitor for copper metal.

According to the values of E_{corr}, β_a, and β_c in Table 3, the addition of the Cefazolin drug to the corrosive medium affects not only the reduction of oxygen gas in the cathodic area but also the oxidation of Cu metal in the anodic area. Through physisorption, the Cefazolin molecules and the chloride ions in the corrosion environment create a protective film on the Cu surface. This film reduces the metal contact area with the corrosive medium and suppresses additional Cu^+ oxidation. According to Xu et al. [73], the rich electronic center (N and conjugate rings) of Cefazolin molecule and the Cu^+ ions share the charge and generate the active complex to inhibit the corrosion reaction.

2.9. A Comparison between the Expired Cefazolin Drug and Other Drugs Previously Mentioned

Table 8 compares the examined expired Cefazolin drug with other drugs described throughout the literature for corrosion inhibition. The comparison shows that the expired Cefazolin drug is more efficient than many expired drugs at inhibiting corrosion.

Table 8. The comparison between the tested expired Cefazolin drug and other expired drugs reported in the literature.

Drug Name	Inhibition Efficiency	References
Expired Concor	75.1% at 300 ppm	[74]
Expired Moxifloxacin	69.7% at 300 ppm	[75]
Expired Acetazolamide	81.4% at 300 ppm	[76]
Expired Phenytoin	79.0% at 500 ppm	[77]
Expired Ranitidine	89.0% at 400 ppm	[78]
Expired Doxycycline	68.5% at 200 ppm	[79]
Expired Cephapirin	83.0% at 600 ppm	[80]
Expired Irbesartan	83.0% at 300 ppm	[81]
Expired Cefazolin	87.0% at 300 ppm	This work

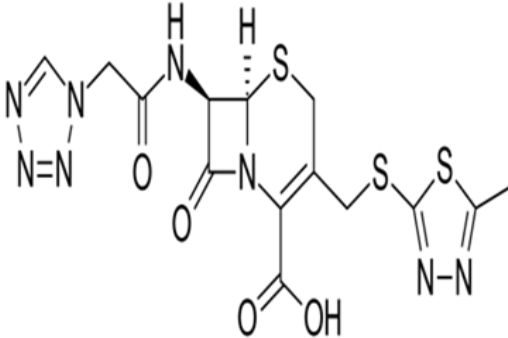## 3. Materials and Methods

3.1. Cu Coupons

The composition (weight%) of the copper metal used in this study was determined by EDX analysis and was found to be 0.031 iron, 0.004 silicon, 0.022 lead, 0.011 nickel, and the rest was Cu.

3.2. Chemicals and Solutions

The Cefazolin structure, IUPAC nomenclature, molecular mass, and molecular formula are shown in Table 9. The employed expired Cefazolin, HCl acid solution, and ethyl alcohol (C_2H_5OH) were purchased from Merck Company of pharmaceuticals (Cairo, Egypt) and used directly.

Table 9. The chemical structure, IUPAC name, molecular mass, and formula of the Cefazolin drug.

Drug	Chemical Structure	Characteristics
Cefazolin		**IUPAC name:** (6R,7R)–3–{[(5–methyl–1,3,4–thiadiazol–2–yl)thio]methyl}–8–oxo–7–[(1H–tetrazol–1–ylacetyl)amino]–5–thia–1–azabicyclo[4.2.0]oct–2–ene–2–carboxylic acid **Molecular Formula:** $C_{14}H_{14}N_8O_4S_3$ **Molecular mass:** 454.51 g/mol

An amount of 1 g of an investigated expired antibiotic was accurately dissolved in 1 L of doubly distilled water to form a stock solution with a concentration of 1000 parts per million (ppm). The stock solution was then diluted to the desired concentration (50–300 ppm) with the appropriate amount of doubly distilled water. High–grade HCl (32 wt.%) was purchased from Sigma-Aldrich (St. Louis, MO, USA). It was diluted with doubly distilled water to prepare the corrosive medium, 0.5 mol L^{-1} HCl.

3.3. WL Method

WL measurements were established according to ASTM–G1 [82]. For twenty–four hours at 298–318 K, copper sheets with dimensions of ($2 \times 2 \times 0.1$ cm^3) were immersed in 0.5 mol L^{-1} HCl without and with different doses of the drug. They were then cleaned, dried, and weighed.

3.4. Electrochemical Measurements

The electrochemical measurements were performed according to ASTM–G102. For PP measurements, a conventional cell with a platinum electrode (counter) and saturated calomel (SCE) as a reference electrode was used [13]. The working Cu rod electrode was pressure–fitted into a polytetrafluoroethylene (PTFE) holder, exposing a surface area of 1 cm^2 to the corrosive medium. The unmasked surface was polished with the emery cloth, cleaned with acetone and distilled water, and then left to dry. An air thermostat was used to take the readings at a constant temperature. By adjusting the copper potential from −0.7 to −0.2 V vs. SCE, the polarization graphs were plotted. A scan rate of 0.2 mV s^{-1} was utilized. Prior to each run, the copper electrode was immersed in the blank solution for 30 min at open circuit potential (OCP) to obtain a steady state.

EIS data were gathered using a sine wave of 10 mV over a wide frequency limit of 100 kHz to 5×10^{-4} Hz. A corrosion program was connected to Volta Lab 40 Potentiostat PGZ 301 for measuring. The copper electrode was fixed at the OCP for 30 min in the examined solution before the impedance spectra were recorded. Two frequencies, 2 and 5 Hz, were used for the EFM study. The waveform renewed at the lowest frequency of 0.1 Hz every second. Current responses associated with harmonic current peaks and inter–modification current peaks were included in the spectrum [83]. The larger peaks were used to calculate the Tafel slopes (β_c and β_a), corrosion current, and causality factors (CF–2 and CF–3).

3.5. Surface Examination

The copper coupons were immersed in a blank solution containing 300 ppm of the expired drug for 8 h to create the adsorbed film. The coupons were then withdrawn and dried. Both SEM and EDX techniques were used to analyze the surface film. Joel JSM–6510 LV SEM was used to test the metal surface after 8 h of immersion in a 0.5 mol L^{-1} HCl solution without and with the drug. The elemental analysis of the copper surface was performed using EDX technique (EDX–FEI–QUANTA FEG 250).

3.6. Computational Studies

A simulation explained the mechanism of adsorption using quantum chemistry. The quantum chemical features were related to the stated inhibitory effectiveness of the tested corrosion inhibitor. DFTB +1.3 was used in the quantum calculation package. The empirical parameters used for integral evaluation in the DFTB calculation were taken from Slater–Koster file libraries. Auorg parameters were used for the present system [84–86]. The IE of Cefazolin was evaluated by calculating several electronic and thermodynamic parameters, such as the adsorption energy, the energy of the highest occupied molecular orbital (E_{HOMO}), the energy of the lowest unoccupied molecular orbital (E_{LUMO}), and the energy gap (ΔE).

A Monte Carlo (MC) simulation investigated the preferential adsorption configurations of Cefazolin molecules on adsorption sites of the periodic structure of copper. Possible adsorption sites were identified by carrying out MC searches of the possible substrate–

adsorbate configurations using a simulated annealing algorithm [84]. MC was performed in a periodic slab model box of super unit cells with a vacuum layer of 20 Å to avoid interaction between periodic unit cells. A single–molecule inhibitor covered a super cell of a copper (111) surface with 9 atomic layers. The compass force field was used to describe the behavior of the Cefazolin molecule on the copper surface during adsorption, as well as the mechanism of interactions involving the molecule and the metal surface.

4. Conclusions

The expired Cefazolin drug effectively inhibited the corrosion of copper metal in 0.5 mol L^{-1} HCl. Potentiodynamic polarization, electrochemical frequency modulation, weight loss, and EIS techniques were used to evaluate the performance of the Cefazolin drug as a protective film. There was good agreement between the weight loss method and the potentiodynamic polarization, electrochemical frequency modulation, and EIS techniques. In 0.5 mol L^{-1} HCl media, Cefazolin showed remarkable inhibition efficiency for copper. The anticorrosion performance enhanced with increasing the concentration of Cefazolin drug, attaining 87% efficiency at 300 ppm, although it decreased at higher temperatures. The inhibition was mainly caused by the adsorption of the expired drug on the copper surface. The adsorption matched the Temkin model. The thermodynamic parameters suggested the physisorption of the drug, forming a protective film on the copper surface. Cefazolin drug is a mixed–type inhibitor. The micrographs and spectra obtained from the SEM and EDX analyses, respectively, supported these findings. DFTB and MC simulation results indicated that the expired drug highly bound to the copper surface via the lone pair of electrons on the heteroatoms, in addition to the π–electrons of the tetrazole ring. The adsorption energy between the drug and copper surface was -459.38 kJ mol^{-1}.

References

1. Esmaily, M.; Svensson, J.E.; Fajardo, S.; Birbilis, N.; Frankel, G.S.; Virtanen, S.; Arrabal, R.; Thomas, S.; Johansson, L.G. Fundamentals and Advances in Magnesium Alloy Corrosion. *Prog. Mater. Sci.* **2017**, *89*, 92–193. [CrossRef]
2. López–Ortega, A.; Bayón, R.; Arana, J.L. Evaluation of Protective Coatings for Offshore Applications. Corrosion and Tribocorrosion Behavior in Synthetic Seawater. *Surf. Coat. Technol.* **2018**, *349*, 1083–1097. [CrossRef]
3. Kolawole, F.O.; Kolawole, S.K.; Agunsoye, J.O.; Adebisi, J.A.; Bello, S.A.; Hassan, S.B. Mitigation of Corrosion Problems in API 5L Steel Pipeline—A Review. *J. Mater. Environ. Sci.* **2018**, *9*, 2397–2410.
4. Abdallah, M.; Asghar, B.H.; Zaafarany, I.; Fouda, A.S. The Inhibition of Carbon Steel Corrosion in Hydrochloric Acid Solution Using some Phenolic Compounds. *Int. J. Electrochem. Sci.* **2012**, *7*, 282–304. [CrossRef]
5. Singh, A.; Ebenso, E.E.; Qurashi, M.A. Corrosion Inhibition of Carbon Steel in HCl Solution by some Plant Extracts. *Int. J. Corros.* **2012**, *2012*, 897430. [CrossRef]
6. Rozenfeld, I.L. *Corrosion Inhibitors*; McGraw–Hill: New York, NY, USA, 1981.

7. Soltani, N.; Tavakkoli, N.; Ghasemi, M. Corrosion Inhibition of Low Carbon Steel by C Nux–Vomica Extract as Green Corrosion Inhibitor in Hydrochloric Acid Solution. *Int. J. Electrochem. Sci.* **2016**, *11*, 8827–8847. [CrossRef]

8. Yaro, A.S.; Khadom, A.A.; Ibraheem, H.F. Peach Juice as an Anti–Corrosion Inhibitor of Mild Steel. *Anti–Corros. Methods Mater.* **2011**, *5*, 116–124. [CrossRef]

9. Yaro, A.S.; Khadom, A.A.; Wael, R.K. Apricot Juice as Green Corrosion Inhibitor of Mild Steel in Phosphoric Acid. *Alexandria Eng. J.* **2013**, *52*, 129–135. [CrossRef]

10. Yaro, A.S.; Khadom, A.A.; Wael, R.K. Garlic Powder as a Safe Environment Green Corrosion Inhibitor for Mild Steel in Acidic Media; Adsorption and Quantum Chemical Studies. *J. Chin. Chem. Soc.* **2014**, *61*, 615–623. [CrossRef]

11. Fontana, M.G.; Green, N.D. *Corrosion Engineering*; McGraw–Hill: New York, NY, USA, 1986.

12. Kamel, M.M.; Rashwan, S.M.; Mahmoud, M.A.; El–Mekawy, S.A.; Awad, M.K.; Ibrahim, H.E. Resorcinol Derivative as an Environmentally Friendly Low Carbon Steel Inhibitor in HCl Medium. *ACS Omega* **2022**, *7*, 17609–17619. [CrossRef]

13. Hegazy, M.A.; Rashwan, S.M.; Meleek, S.; Kamel, M.M. Synthesis, Characterization and Mitigation Action of Innovative Schiff Base on Steel Disintegration in Sulfuric Acid Solution. *Mater. Chem. Phys.* **2021**, *267*, 124697. [CrossRef]

14. Al–Najjar, S.S.; Al–Baitai, A.Y. Synthesized of Novel Imidazole–derived Schiff Base as a Corrosion Inhibitor of Carbon Steel in Acidic Medium Supported by Electrochemical and DFT Studies. *Phys. Chem. Res.* **2022**, *10*, 179–194.

15. Antonijevic, M.M.; Milić, S.M.; Petrović, M.B. Films Formed on Copper Surface in Chloride Media in the Presence of Azoles. *Corros. Sci.* **2009**, *51*, 1228–1237. [CrossRef]

16. Sherif, E.S.M.; Erasmus, R.; Comins, J. Inhibition of Copper Corrosion in Acidic Chloride Pickling Solutions by 5–(3–Aminophenyl)−Tetrazole as a Corrosion Inhibitor. *Corros. Sci.* **2008**, *50*, 3439–3445. [CrossRef]

17. Cano, E.; Polo, J.; La Iglesia, A.; Bastidas, J. A Study on the Adsorption of Benzotriazole on Copper in Hydrochloric Acid Using the Inflection Point of the Isotherm. *Adsorption* **2004**, *10*, 219–225. [CrossRef]

18. Askari, M.; Aliofkhazraei, M.; Ghaffari, S.; Hajizadeh, A. Film Former Corrosion Inhibitors for Oil and Gas Pipelines—A Technical Review. *J. Nat. Gas Sci. Eng.* **2018**, *58*, 92–114. [CrossRef]

19. Pathak, R.K.; Mishra, P. Drugs as Corrosion Inhibitors: A Review. *Inter. J. Sci. Res.* **2016**, *5*, 669–671.

20. Gikonyo, D.; Gikonyo, A.; Luvayo, D.; Ponoth, P. Drug Expiry Debate: The Myth and the Reality. *Afr. Health Sci.* **2019**, *19*, 2737–2739. [CrossRef]

21. Vaszilcsin, N.; Kellenberger, A.; Dan, M.L.; Duca, D.A.; Ordodi, V.L. Efficiency of Expired Drugs Used as Corrosion Inhibitors: A Review. *Materials* **2023**, *16*, 5555. [CrossRef]

22. Alamry, A.A.; Khan, A.; Aslam, J.; Haussien, M.A. Corrosion Inhibition of Mild Steel in Hydrochloric Acid Solution by the Expired Ampicillin Drug. *Sci. Rep.* **2023**, *13*, 6724. [CrossRef]

23. Sundaram, R.G.; Vengatesh, G.; Sundaravadivelu, M. Surface Morphological and Quantum Chemical Studies of some Expired Drug Molecules as Potential Corrosion Inhibitors for Mild Steel in Chloride Medium. *J. Surf. Interface* **2021**, *22*, 100841. [CrossRef]

24. Zakaria, K.; Abbas, M.A.; Bedair, M.A. Herbal Expired Drug Bearing Glycosides and Polysaccharides Moieties as Green and Cost–effective Oilfield Corrosion Inhibitor: Electrochemical and Computational Studies. *J. Mol. Liq.* **2022**, *352*, 118689. [CrossRef]

25. Alfakeer, M.; Abdallah, M.; Fawzy, A. Corrosion Inhibition Effect of Expired Ampicillin and Flucloxacillin Drugs for Mild Steel in Aqueous Acidic Medium. *Int. J. Electrochem. Sci.* **2020**, *15*, 3283–3297. [CrossRef]

26. Abdallah, M.; Fawzy, A.; Al Bahir, A. The Effect of Expired Acyclovir and Omeprazole Drugs on the Inhibition of Sabic Iron Corrosion in HCl Solution. *Int. J. Electrochem. Sci.* **2020**, *15*, 4739–4753. [CrossRef]

27. Raghavendra, N.V.; Hublikar, L.V.; Ganiger, P.J.; Bhinge, A.S. Expired Ceftin as a Corrosion Inhibitor for Mild Steel in 5% HCl Solution. *Int. J. Green Herbal Chem.* **2019**, *8*, 610–616.

28. Njoku, C.N.; Enendu, B.N.; Okechukwu, S.J.; Igboko, N.; Anyikwa, S.O.; Ikeuba, A.I.; Onyeachu, I.B.; Etim, I.N.; Demian, I.; Njoku, D.I. Review on Anti–Corrosion Properties of Expired Antihypertensive Drugs as Benign Corrosion Inhibitors for Metallic Materials in Various Environments. *Results Eng.* **2023**, *18*, 101183. [CrossRef]

29. Abdallah, A.; Soliman, K.A.; Alfakeer, M.; Hawsawi, H.; Mohsen Al–bonayan, A.; Al–Juaid, S.S.; Salah Abd El Wanees, S.A.; Motawea, M.S. Expired Antifungal Drugs as Effective Corrosion Inhibitors for Carbon Steel in 1 M HCl Solution: Practical and Theoretical Approaches. *ASC Omega* **2023**, *8*, 34516–34533. [CrossRef]

30. Ibrahim, M.A.A.; Moussa, N.A.M.; Mahmoud, A.H.M.; Sayed, S.R.M.; Sidhom, P.A.; Abd El–Rahman, M.K.; Shoeib, T.; Mohamed, L.A. Density Functional Theory Study of The Corrosion Inhibition Performance of 6–Mercaptopurine and 6–thioguanine Expired Drugs toward the Aluminum (111) Surface. *RSC Adv.* **2023**, *13*, 29023. [CrossRef]

31. Montaser, A.A.; El–Mahdy, M.S.; Elsayed, E.E.; Mahmoud, E.E.E.; Fouda, A.S. Recycling of Expired Ciprofloxacin in Synthetic Acid Rain (SAR) Solution as A Green Corrosion Inhibitor for Copper: A Theoretical and Experimental Evaluation. *J. Appl. Electrochem.* **2024**, *54*, 439–456. [CrossRef]

32. Feng, L.; Zhang, S.; Rongkai Pan, Y.Z.; Du, H.; Liu, F.; Yang, Y. Expired Glucosamine Drugs as Green Corrosion Inhibitors for Carbon Steel in H_2SO_4 Solution and Synergistic Effect of Glucosamine Molecules with Iodide Ions: Combined Experimental and Theoretical Investigations. *Crystals* **2023**, *13*, 205. [CrossRef]

33. Lin, Q.; Zhang, Q.; Huang, Y.; Luo, Y.; Zhang, R.; Guo, L. Expired Flunarizine Hydrochloride as Corrosion Inhibitors for Q235 Steel in Hydrochloric Acid Medium: Experimental and Computational Investigation. *Surf. Interface Anal.* **2023**, *55*, 774–786. [CrossRef]

34. Kasim Sheit, H.M.; Musthafa Kani, S.; Anwar Sathiq, M.; Syed Abuthahir, S.S.; Subhapriya, P.; Nivedhitha, K.S.; Umarfarooq, M.A.; Badruddin, I.B.; Kamangar, S.; Shaik, A.S. Experimental Studies on the Effect of Expired Amiodarone Drug (EAD) as a Corrosion Inhibitor on Mild Steel in 1 M HCl. *Materials* **2024**, *17*, 75.

35. Hamza, R.A.; Samawi, K.A.; Salman, T.A. Inhibition Studies of Aluminium Alloy (2024) Corrosion in Acid Hydrochloride Solution Using an Expired Phenylphrine Drug. *Egypt. J. Chem.* **2020**, *63*, 2863–2875.

36. Attar, T.; Benchadli, A. Studying the Effectiveness of an Expired Betamethasone Drug in Sulfuric Acid Solutions to Examine the Corrosive Behavior of Copper Using Weight Loss and Experimental Design. *J. Turk. Chem. Soc. Sect. A Chem.* **2024**, *11*, 291–302. [CrossRef]

37. Dohare, P.; Chauhan, D.S.; Quraishi, M.A. Expired Podocip Drug as Potential Corrosion Inhibitor for Carbon Steel in Acid Chloride Solution. *Int. J. Corros. Scale Inhib.* **2018**, *7*, 25–37.

38. Srinivasulu, A.; Kasthuri, P.K. Study of Inhibition and Adsorption Properties of Mild Steel Corrosion by Expired Pharmaceutical Gentamicin Drug in Hydrochloric Acid Media. *Orient. J. Chem.* **2017**, *33*, 2616–2624. [CrossRef]

39. Abdel Hameed, R.S.; Essa, A.; Nassar, A.; Magd Badr, M.; Huwaimel, B.; Al–Mhyawi, S.R.; Alshammary, F.; Abu Seni, A.; Abdallah, M. Chemical and Electrochemical Studies on Expired Lioresal Drugs as Corrosion Inhibitors for Carbon Steel in Sulfuric Acid. *J. New Mat. Electrochem. Syst.* **2022**, *25*, 268–276. [CrossRef]

40. Kellenberger, A.; Duca, D.A.; Dan, M.L.; Medeleanu, M. Recycling Unused Midazolam Drug as Efficient Corrosion Inhibitor for Copper in Nitric Acid Solution. *Materials* **2022**, *15*, 2918. [CrossRef] [PubMed]

41. Raghavendra, N.; Hublikar, L.V.; Bhinge, A.S.; Ganiger, P.J. Corrosion Inhibition Property of Expired Fluoxymesterone Drug on the Aluminum (Al) Surface in 3 % NaCl Solution. *Int. J. Curr. Pharm. Res.* **2019**, *11*, 48–50. [CrossRef]

42. Priyanka Singh, P.; Chauhan, D.S.; Srivastava, K.; Srivastava, V.; Quraishi, M.A. Expired Atorvastatin Drug as Corrosion Inhibitor for Mild Steel in Hydrochloric Acid Solution. *Int. J. Ind. Chem.* **2017**, *8*, 363–372. [CrossRef]

43. Birkhead, H.A.; Briggs, G.B.; Saunders, L.Z. Toxicology of Cefazolin in Animals. *J. Infec. Dis.* **1973**, *128* (Suppl. 2), S379–S381. [CrossRef]

44. Hegazy, M.A. Novel Cationic Surfactant Based on Triazole as a Corrosion Inhibitor for Carbon Steel in Phosphoric Acid Produced by Dihydrate Wet Process. *J. Mol. Liq.* **2015**, *208*, 227–236. [CrossRef]

45. Bobina, M.; Kellenberger, A.; Millet, J.P.; Muntean, C.; Vaszilcsin, N. Corrosion Resistance of Carbon Steel in Weak Acid Solutions in the Presence of l–Histidine as Corrosion Inhibitor. *Corros. Sci.* **2013**, *69*, 389–395. [CrossRef]

46. Sherif, E.M. Corrosion Behavior of Copper in 0.50 M Hydrochloric Acid Pickling Solutions and its Inhibition by 3–amino–1, 2, 4–triazole and 3–amino–5–mercapto–1, 2, 4–triazole. *Int. Electrochem. Sci.* **2012**, *7*, 1884–1897. [CrossRef]

47. Zhang, D.Q.; Gao, L.X.; Zhou, G.D. Inhibition of Copper Corrosion by bis–(1–Benzotriazolymethylene)−(2,5–Thiadiazoly)−disulfide in Chloride Media. *J. Appl. Surf. Sci.* **2004**, *225*, 287–293. [CrossRef]

48. El Warraky, A.A.; El Shayeb, H.A.E.; Sherif, E.M. Pitting Corrosion of Copper in Chloride Solutions. *Anti–Corros. Methods Mater.* **2004**, *51*, 52–61. [CrossRef]

49. Ita, B.I.; Offiong, O.E. The Study of the Inhibitory Properties of Benzoin, Benzil, Benzoin–(4–phenylthiosemicarbazone) and Benzyl–(4–phenylthiosemi carbazone) on the Corrosion of Mild Steel in Hydrochloric Acid. *Mater. Chem. Phys.* **2001**, *70*, 330–335. [CrossRef]

50. Khaled, K.F. New Synthesized Guanidine Derivative as a Green Corrosion Inhibitor for Mild Steel in Acidic Solutions. *Int. J. Electrochem. Sci.* **2008**, *3*, 462–475. [CrossRef]

51. Fouda, A.S.; El–desoky, A.M.; Nabih, A. Inhibitive, Adsorption, Synergistic Studies on Copper Corrosion in Nitric Acid Solutions by some Organic Derivatives. *Adv. Mater. Corros.* **2013**, *2*, 1–15.

52. Najem, A.; Campos, O.S.; Girst, G.; Raji, M.; Hunyadi, A.; García–Antón, J.; Bellaouchou, A.; Amin, H.M.A.; Boudalia, M. Experimental and DFT Atomistic Insights into the Mechanism of Corrosion Protection of Low–Carbon Steel in an Acidic Medium by Polymethoxyflavones from Citrus Peel Waste. *J. Electrochem. Soc.* **2023**, *170*, 093512. [CrossRef]

53. Kamel, M.M.; Mohsen, Q.; Anwer, Z.M.; Sherif, M.A. An Expired Ceftazidime Antibiotic as an Inhibitor for Disintegration of Copper Metal in Pickling HCl Media. *J. Mater. Res. Technol.* **2021**, *11*, 875–886. [CrossRef]

54. Tan, B.; Xiang, B.; Zhang, S.; Qiang, Y.; Xu, L.; Chen, S.; He, J. Papaya Leaves Extract as a Novel Eco–friendly Corrosion Inhibitor for Cu in H_2SO_4 Medium. *J. Colloid Interface Sci.* **2021**, *582*, 918–931. [CrossRef] [PubMed]

55. Tan, B.; He, J.; Zhang, S.; Xu, C.; Chen, S.; Liu, H.; Li, W. Insight into Anti–corrosion Nature of *Betel* Leaves Water Extracts as the Novel and Eco–friendly Inhibitors. *J. Colloid Interface Sci.* **2021**, *585*, 287–301. [CrossRef] [PubMed]

56. Singh, A.K.; Quraishi, M.A. Effect of Cefazolin on the Corrosion of Mild Steel in HCl Solution. *Corros. Sci.* **2010**, *52*, 152–160. [CrossRef]

57. Qiang, Y.; Zhang, S.; Yan, S.; Zou, X.; Chen, S. Three Indazole Derivatives as Corrosion Inhibitors of Copper in a Neutral Chloride Solution. *Corros. Sci.* **2017**, *126*, 295–304. [CrossRef]

58. Lebrini, M.; Lagrenee, M.; Vezin, H.; Gengembre, L.; Bentiss, F. Electrochemical and Quantum Chemical Studies of New Thiadiazole Derivatives Adsorption on Mild Steel in Normal Hydrochloric Acid Medium. *Corros. Sci.* **2005**, *47*, 485–505. [CrossRef]

59. Govindasamy, R.; Ayappan, S. Study of Corrosion Inhibition Properties of Novel Semicarbazones on Mild Steel in Acidic Solutions. *J. Chil. Chem. Soc.* **2015**, *60*, 2786–2798. [CrossRef]

60. Eddahhaoui, F.Z.; Najem, A.; Elhawary, M.; Boudalia, M.; Campos, O.S.; Tabyaoui, M.; Garcia, A.J.; Bellaouchou, A.; Amin, H.M.A. Experimental and Computational Aspects of Green Corrosion Inhibition for Low Carbon Steel in HCl Environment Using Extract of Chamaerops Humilis Fruit Waste. *J. Alloys Compds.* **2024**, *977*, 173307. [CrossRef]

61. Sekine, I.; Sabongi, M.; Hagiuda, H.; Oshibe, T.; Yuasa, M.; Imahama, T.; Shibata, Y.; Wake, T. Corrosion Inhibition of Mild Steel by Cationic and Anionic Polymers in Cooling Water System. *J. Electrochem. Soc.* **1992**, *139*, 3167–3173. [CrossRef]

62. Hegazy, M.A.; Atlam, F.M. Three Novel Bola Amphiphiles as Corrosion Inhibitors for Carbon Steel in Hydrochloric Acid: Experimental and Computational Studies. *J. Mol. Liq.* **2016**, *218*, 649–662. [CrossRef]

63. Lebrini, M.; Lagrenee, M.; Traisnel, M.; Gengembre, L.; Vezin, H.; Bentiss, F. Enhanced Corrosion Resistance of Mild Steel in Normal Sulfuric Acid Medium by 2,5–bis(n–thienyl)$-$1,3,4–thiadiazoles: Electrochemical, X–ray Photoelectron Spectroscopy and Theoretical Studies. *Appl. Surf. Sci.* **2007**, *253*, 9267–9276. [CrossRef]

64. Tan, B.; Zhang, S.; Qiang, Y.; Guo, L.; Feng, L.; Liao, C. A Combined Experimental and Theoretical Study of the Inhibition Effect of Three Disulfide–based Flavouring Agents for Copper Corrosion in 0.5 M Sulfuric Acid. *J. Colloid Interface Sci.* **2018**, *526*, 268–280. [CrossRef] [PubMed]

65. Jennane, J.; Ebn Touhami, M.; Zehra, S.; Baymou, Y.; Kim, S.H.; Chung, I.M.; Lgaz, H. Influence of Sodium Gluconate and Cetyltrimethylammonium Bromide on the Corrosion Behavior of Duplex (α–β) Brass in Sulfuric Acid Solution. *Mater. Chem. Phys.* **2019**, *227*, 200–210. [CrossRef]

66. Nasser, A.; EL Basiony, N.M.; Migahed, M.A.; Abd–El–Bary, H.M.; Mohamed, T.A. Experimental and Theoretical Insights into Synthesized Gemini Corrosion Inhibitor for X65–Steel in 1M HCl. *Egypt. J. Chem.* **2022**, *65*, 845–867.

67. Pais, M.; Rao, P. Electrochemical, Spectroscopic and Theoretical Studies for Acid Corrosion of Zinc Using Glycogen. *Chem. Pap.* **2021**, *75*, 1387–1399. [CrossRef]

68. Chakraborty, T.; Gazi, K.; Ghosh, D.C. Computation of the Atomic Radii through the Conjoint Action of the Effective Nuclear Charge and the Ionization Energy. *Mol. Phys.* **2010**, *108*, 2081–2092. [CrossRef]

69. Singh, A.; Ansari, K.R.; Kumar, A.; Liu, W.; Songsong, C.; Lin, Y. Electrochemical, Surface and Quantum Chemical Studies of Novel Imidazole Derivatives as Corrosion Inhibitors for J55 Steel in Sweet Corrosive Environment. *J. Alloys Compd.* **2017**, *712*, 121–133. [CrossRef]

70. Khalil, N. Quantum Chemical Approach of Corrosion Inhibition. *Electrochim. Acta* **2003**, *48*, 2635–2640. [CrossRef]

71. El Basiony, N.; Elgendy, A.; El–Tabey, A.E.; Al Sabagh, A.; Abd El–Hafez, G.M.; Abd El–raouf, M.; Migahed, M. Synthesis, Characterization, Experimental and Theoretical Calculations (DFT, and MC) of Ethoxylated Aminothiazole as Inhibitor for X65 Steel Corrosion in Highly Aggressive Acidic Media. *J. Mol. Liq.* **2020**, *297*, 111940. [CrossRef]

72. Guo, L.; Ren, X.; Zhou, Y.; Xu, S.; Gong, Y. Monte Carlo Simulations of Corrosion Inhibition of Copper by Two Schiff Bases. In *International Conference on Materials, Environmental and Biological Engineering (MEBE 2015)*; Atlantis Press: Amsterdam, The Netherlands, 2015. [CrossRef]

73. Xu, C.; Tan, B.; Zhang, S.; Li, W. Corrosion Inhibition of Copper in Sulfuric Acid by Leonurus Japonicas Houtt, Extract as a Green Corrosion Inhibitor: Combination of Experimental and Theoretical Research. *J. Taiwan Inst. Chem. Eng.* **2022**, *139*, 104532. [CrossRef]

74. Fouda, A.S.; El–Azaly, A.M. Expired Concor Drug as Potential Non–toxic Corrosion Inhibitor for 304 Stainless Steel in Hydrochloric Acid Solution. *Zastita Materijala* **2018**, *59*, 226–236. [CrossRef]

75. Hussin, A.; Abdel Hameed, R.S.; Ali, F.A.; Aboul Magd, A.S.; Salah, M. Effect of Expired Drugs as Corrosion Inhibitors for Carbon Steel in 1M HCl Solution. *Int. J. Pharm. Sci. Rev. Res.* **2014**, *27*, 146–152.

76. Chaudhari, L.P.; Patel, S.N. Corrosion Inhibition Study of Expired Acetazolamide on Mild Steel in Dilute Hydrochloric Acid Solution. *J. Bio. Tribo. Corros.* **2019**, *5*, 20. [CrossRef]

77. Reza, I.; Saleemi, A.R.; Naveed, S. Corrosion Inhibition of Mild Steel in HCl Solution by Tinidazole. *Pol. J. Chem. Technol.* **2011**, *13*, 67–71. [CrossRef]

78. Abdel Hameed, R.S. Ranitidine Drugs as Non–toxic Corrosion Inhibitors for Mild Steel in Hydrochloric Acid Medium. *Port. Electrochim. Acta.* **2011**, *29*, 273–285. [CrossRef]

79. Rotaru, I.; Varvara, S.; Gaina, L.; Muresan, L.M. Antibacterial Drugs as Corrosion Inhibitors for Bronze Surfaces in Acidic Solutions. *Appl. Surf. Sci.* **2014**, *321*, 188–196. [CrossRef]

80. El–Haddad, M.N.; Fouda, A.S.; Hassan, A.F. Data from Chemical, Electrochemical and Quantum Chemical Studies for Interaction Between Cephapirin Drug as an Eco–friendly Corrosion Inhibitor and Carbon Steel Surface in Acidic Medium. *Chem. Data Collect.* **2019**, *22*, 100251. [CrossRef]

81. Srivastava, M.; Tiwari, P.; Srivastava, S.K.; Prakash, R.; Ji, G. Electrochemical Investigation of Irbesartan Drug Molecules as an Inhibitor of Mild Steel Corrosion in 1M HCl and 0.5 M H_2SO_4 Solutions. *J. Mol. Liq.* **2017**, *236*, 184–197. [CrossRef]

82. *Designation: G 1–03*; Standard Practice for Preparing, Cleaning, and Evaluating Corrosion Test Specimens. ASTM International: West Conshohocken, PA, USA, 1990; pp. 19428–22959.

83. Bosch, R.W.; Hubrecht, J.; Bogaerts, W.F.; Syrett, B.C. Electrochemical Frequency Modulation: A New Electrochemical Technique for Online Corrosion Monitoring. *Corrosion* **2001**, *57*, 60–70. [CrossRef]

84. Frenkel, D.; Smit, B. *Understanding Molecular Simulation: From Algorithms to Applications*; Academic Press: San Diego, CA, USA, 2002.

85. Fihey, A.; Hettich, C.; Touzeau, J.; Maurel, F.; Perrier, A.; Köhler, C.; Aradi, B.; Frauenheim, T. Complexes of Gold and Imidazole Formed in Helium Nanodroplets. *J. Comput. Chem.* **2015**, *36*, 2075–2087. [CrossRef] [PubMed]

86. Zheng, G.; Witek, H.A.; Bobadova–Parvanova, P.; Irle, S.; Musaev, D.G.; Prabhakar, R.; Morokuma, K.; Lundberg, M.; Elstner, M.; Köhler, C.; et al. Modeling Dynamical Phenomena in Fe(II) Dyes and Dye–semiconductor Assemblies. *J. Chem. Theory Comput.* **2007**, *3*, 1349–1367. [CrossRef] [PubMed]